frontiers | Frontiers in Marine Science

ORIGINAL RESEARCH
published: 13 May 2022
doi: 10.3389/fmars.2022.843295

Cracking and Photo-Oxidation of Polyoxymethylene Degraded in Terrestrial and Simulated Marine Environments

Chih-Cheng Tang[1,2], *Ying-Ting Chen*[1], *Yi-Ming Zhang*[1], *Huey-Ing Chen*[3], *Peter Brimblecombe*[1] *and Chon-Lin Lee*[1,4,5,6*]

[1] Department of Marine Environment and Engineering, National Sun Yat-sen University, Kaohsiung, Taiwan, [2] Learning Guidance Center, Open University of Kaohsiung, Kaohsiung, Taiwan, [3] Department of Chemical Engineering, National Cheng Kung University, Tainan, Taiwan, [4] Department of Public Health, College of Health Science, Kaohsiung Medical University, Kaohsiung, Taiwan, [5] Aerosol Science and Research Center, National Sun Yat-sen University, Kaohsiung, Taiwan, [6] Department of Applied Chemistry, Providence University, Taichung, Taiwan

Marine plastic debris is an environmental problem, and its degradation into microplastics (1-5000 μm) introduces them into the food chain. In this study, small polyoxymethylene (global production ~3000 Tg per year) pellets were exposed in terrestrial and simulated marine environments to heat and light, resulting in cracking during decay with increasing IR absorption (OH-bonds). Furthermore, sunlight over three years reduced pellet mass and diameter (~10% and ~40%), initially yielding 100-300 μm fragments. Changes under UV irradiation were smaller as it could not penetrate into particle interiors. Characteristic spacing of surface striations (100-300 μm) initiated radial cracks to pellet interiors, and breakdown ultimately meant 95% of particles were <300 μm, which are potentially incorporated in marine turbidites.

Keywords: fragmentation, marine debris, microplastics, surface cracking, pellets

OPEN ACCESS

Edited by:
Ana Isabel Catarino,
Flanders Marine Institute, Belgium

Reviewed by:
Tadele Assefa Aragaw,
Bahir Dar University, Ethiopia
Lisbet Sørensen,
SINTEF Ocean, Norway
Zhiyue Niu,
Flanders Marine Institute, Belgium

***Correspondence:**
Chon-Lin Lee
linnohc@fac.nsysu.edu.tw

Specialty section:
This article was submitted to Marine Pollution, a section of the journal Frontiers in Marine Science

Received: *25 December 2021*
Accepted: *31 March 2022*
Published: *13 May 2022*

Citation:
Tang C-C, Chen Y-T, Zhang Y-M, Chen H-I, Brimblecombe P and Lee C-L (2022) Cracking and Photo-Oxidation of Polyoxymethylene Degraded in Terrestrial and Simulated Marine Environments. Front. Mar. Sci. 9:843295. doi: 10.3389/fmars.2022.843295

HIGHLIGHTS

- Polyoxymethylene pellets in sunlight fragment with deep cracks ~225 μm
- Fragmentation is stronger than in polyvinylchloride or polypropylene pellets
- UV degradation is revealed as surface crazing
- Fragmentation leads to particles 100-300 μm, which subsequently become smaller
- Degradation reveals increases in OH bonds

INTRODUCTION

Polyoxymethylene (POM) products end up as marine plastic debris and occur in the benthos arising from land or ocean-based sources (Sfriso et al., 2020). Liu et al. (2021) found POM microplastics present in water, sediment, and fish samples from the Dafeng River, a remote river in China. The polymer is an attractive engineering material with favorable mechanical properties, wear resistance,

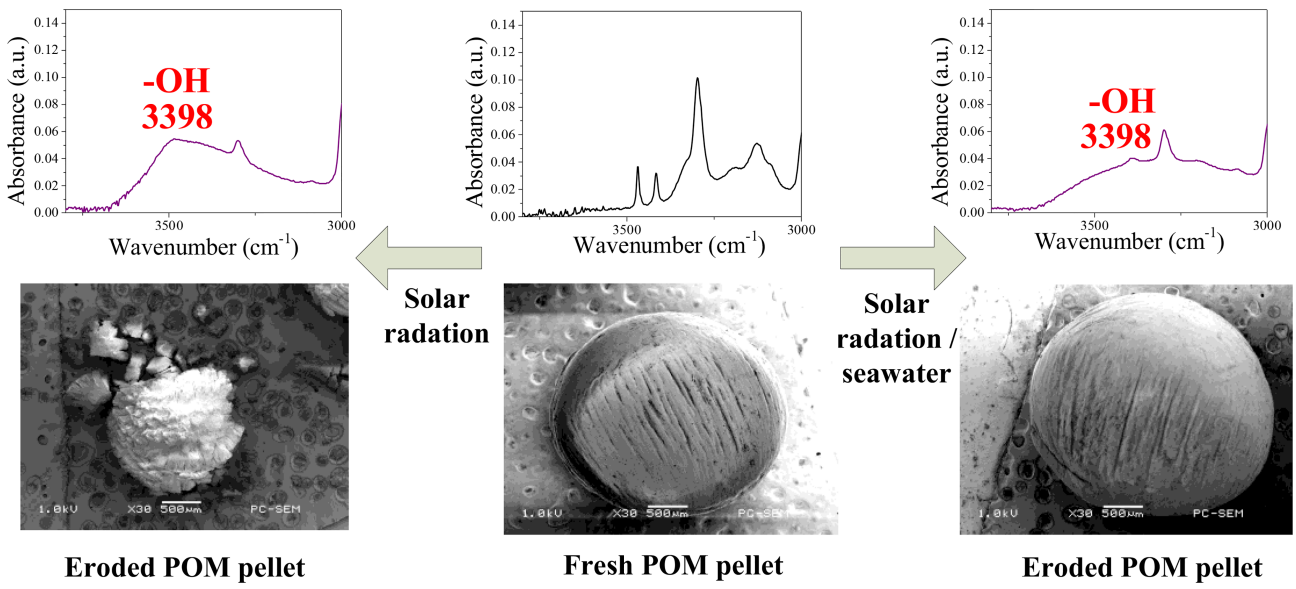

GRAPHICAL ABSTRACT | Graphical Abstract for Tang C-C, Chen Y-T, Zhang Y-M, Chen H-I, Brimblecombe P and Lee C-L (2022) Cracking and Photo-Oxidation of Polyoxymethylene Degraded in Terrestrial and Simulated Marine Environments. Front. Mar. Sci. 9:843295. doi: 10.3389/fmars.2022.843295.

dimensional stability, chemical resistance and electrical insulation so has been used not only in the automotive and mechanical industries, electronics, consumer goods and home appliances, but also as a surgical implant material and in medical devices and drug delivery systems (Vilà Ramirez et al., 2009; Zhang et al., 2018; Król-Morkisz et al., 2019). Marine plastic waste suffers thermal-, photo-, chemical- and bio- degradation breaking into micro- (<5 mm) and nano (<1,000 nm) contaminants, which can be related to the physical and molecular properties (Alimi et al., 2018; Coyle et al., 2020; Gangadoo et al., 2020; Kavya et al., 2020; Min et al., 2020; Napper and Thompson, 2020).

Release of microplastics from larger plastic fragments, particularly those which accumulate on the sea surface microlayer are typically non-biodegradable and sorb toxic organic and inorganic compounds (Bakir et al., 2014; Song et al., 2014; Hermabessiere et al., 2017; Carbery et al., 2018; Hahladakis et al., 2018; Huffer et al., 2018; Wang et al., 2018; Barletta et al., 2019; Naik et al., 2020). Finally, the action of fouling alters the overall buoyancy of these particles and leads to their aggregation as marine snow that settles from surface water to seabed, potentially threatening benthic life (Sfriso et al., 2020). As a result, it is increasingly important to understand the potential formation of microplastic fibers and particles in a marine environment (Naik et al., 2020), with denser materials being transferred to deep sediments by turbidity currents (Pohl et al., 2020).

Degradation of marine plastics takes place through mechanical processes along with thermal and photo-oxidative processes (Fotopoulou and Karapanagioti, 2017), which changes their surfaces at the microscopic scale (Tang et al., 2018; Tang et al., 2019). There have been some studies of the accelerated degradation of polyoxymethylene, such as photodegradation and thermal degradation (Cottin et al., 2000; Vilà Ramirez et al., 2009). This plastic is very sensitive to environmental degradation with photo-oxidation leading to the production of molecules such as CO, CO_2, HCOOH, CH_4 and C_2H_6, while photodegradation under vacuum or in an inert atmosphere yields only H_2CO and some CO (Cottin et al., 2000; Kusy and Whitley, 2005; Lüftl et al., 2006; Rabek, 2012); additionally plastic is known to release alkanes in marine environments through degradation (Royer et al., 2018). Crack formation and propagation in POM has been studied, and microscopic examination has identified the breakdown of craze-like structures arising from interlamellar cavitation and which are characteristic of the whole range of test conditions, may relax three-dimensional constraints on regions of matrix that are then able to draw down to form the macro fibrils (Plummer et al., 2000; Plummer, 2004). These processes are at the micron scale, and much smaller than the fragmentation described in the current study. Here, degradation mechanisms, products and the surface morphologies might be very far from what is expected in the marine environment where natural degradation, including photodegradation, thermo-oxidative degradation, hydrolytic degradation and biodegradation by microorganisms is a more complex interaction (Webb et al., 2012).

The primary objective of this research is to monitor the morphology and chemical properties of the emerging plastic material-POM pellets exposed to heat, UVB, and solar radiation in terrestrial and simulated marine environment for long periods of time. It also examines their changing characteristics and suggests probable degradation mechanisms in the natural

environment to explain the affinity of plastic marine debris for trace metals, persistent organic pollutants, and microbes, as well as their tendency for biofouling.

MATERIALS AND METHODS

Materials and Sample Preparation

The POM (FM090®) raw material (~3 mm elliptical shaped pellets) used in this research was supplied by Formosa Plastics Corporation. It has a density of 1.41 g cm^{-3}, a melting point of 165°C as measured by Formosa Plastics Corporation and is widely used in the automotive and consumer electronics industry due to its thermal stability and mechanical strength. American Chemical Society (ACS) grade chemicals and reagents were used in the experiments; while artificial seawater was prepared following the protocols set up by the Marine Biological Laboratory, Woods Hole, MA (http://comm.archive.mbl.edu/BiologicalBulletin/COMPENDIUM/CompTab3.html), with NaCl 423.00 g, KCl 9.00g, $CaCl_2$ 9.27g, $MgCl_2$ 22.94g, $MgSO_4$ 25.50g, * $NaHCO_3$ 2.14g (added last), deionized (DI) water from a Milli-Q system (Millipore, Billerica, MA) to 1L and 200 ppm NaN_3 (antibacterial agent) to prevent biological effects.

Weathering Experiments

The sample code names, and weathering conditions are listed in **Table 1**. POM-Su simulated POM weathering in a sunlit terrestrial environment (Su); while POM-SWSu simulated POM weathering in marine environments (SW) under solar exposure and POM-SWSuN3 with azide (N3) to reduce microbiological effects. These were exposed on the rooftop of the Gushan precinct building of the Kaohsiung City Police Department, Taiwan (22°37'36.0"N 120°16'41.5"E). In this research, POM-Su and POM-SWSuN3 were exposed to sunshine with radiance 338–718 (MJ m^{-2}) for ~8255 h at 10.2–35.6°C, measured by the Central Weather Bureau, Taiwan.

POM-SWN3 simulated seawater-only weathering. The morphology and chemical properties of POM following photo- and thermal-oxidation were monitored with samples: POM-O50, POM-O100. According to the literature, the theoretical maximum possible ground surface temperature is between 90 and 100°C, and the maximum natural ground surface temperature, is 93.9°C. Therefore we examined thermal degradation of POM pellets in a channel drying oven, (OV-452) set at 50°C (O50) and 100°C (O100), for 42 and 36 months (Kubecka, 2001; Mildrexler et al., 2011), designated POM-O50 and POM-O100. POM-U and POM-SWUNa were exposed for 36 months at 25 ± 2°C to radiation below 350 nm under GL20SE ultraviolet B lamps (Sankyo Denki Co., Japan), dry and in artificial seawater. The weathering methods mentioned above were previously used in studies of the degradation of polyvinyl chloride and polypropylene (Tang et al., 2018; Tang et al., 2019).

Pellet characterization

The morphology characteristics of weathered POM samples were observed by environmental scanning electron microscopy (JEOL JSM 6380 SEM), designating three randomly chosen plastic pellets. Image J was used to analyze SEM images, in a supervised mode, to determine fragment area and measures of diameter. The pellets were weighed, and following exposure the remnant material was sieved using a range of sieves, but most frequently those of mesh size 50 (0.297 mm) and 80 (0.177 mm). The dry weight of pellets was measured with a Shimadzu electronic analytical balance ATX224.

Fourier transform infrared spectroscopy (FTIR) was used to determine the original and new functional groups on the surface of three randomly sampled virgin and weathered pellets. The FTIR spectra over the range from 4000 cm^{-1} to 600 cm^{-1} were obtained using a Nicolet 6700 FT-IR system integrated with a Smart Endurance single bounce diamond attenuated total reflectance (ATR) accessory (Nicolet Instrument Corp., Madison, WI) and Thermo Electron Corporation OMNIC software.

Statistical analysis

We often used medians and quartiles: Q1 and Q3 analysis were used to represent central tendency and dispersion as the data were not normally distributed. Correlation at small sample sizes with non-integer values and frequent ties adopted the Kendall rank correlation coefficient, with test statistic τ (Wessa.net). It was used in preference to Spearman's test (test statistic ρ), because it met our needs and as Gilpin (1993) notes, Kendall τ "approaches a normal distribution more rapidly than ρ, as … sample size, increases; and τ is also more tractable mathematically, particularly when ties are present". The Theil-Sen slope was used as a nonparametric

TABLE 1 | A list for samples treated under various exposures.

Sample Name	Photo	Thermal	Artificial Seawater	NaN_3	Time (months)	Site
POM-V	w/o	w/o	w/o	w/o	42	Laboratory
POM-Su	solar	w/o	w/o	w/o	42	Roof top
POM-SWSu	solar	w/o	w	w/o	36	Roof top
POM-SWSuN3	solar	w/o	w	w	42	Roof top
POM-SWN3	w/o	w/o	w	w	36	Laboratory
POM-O50	w/o	50°C	w/o	w/o	42	Laboratory
POM-O100	w/o	100°C	w/o	w/o	30	Laboratory
POM-U	UVB	w/o	w/o	w/o	36	Laboratory
POM- SWUN3	UVB	w/o	w	w	36	Laboratory

w/o – without, w – with.

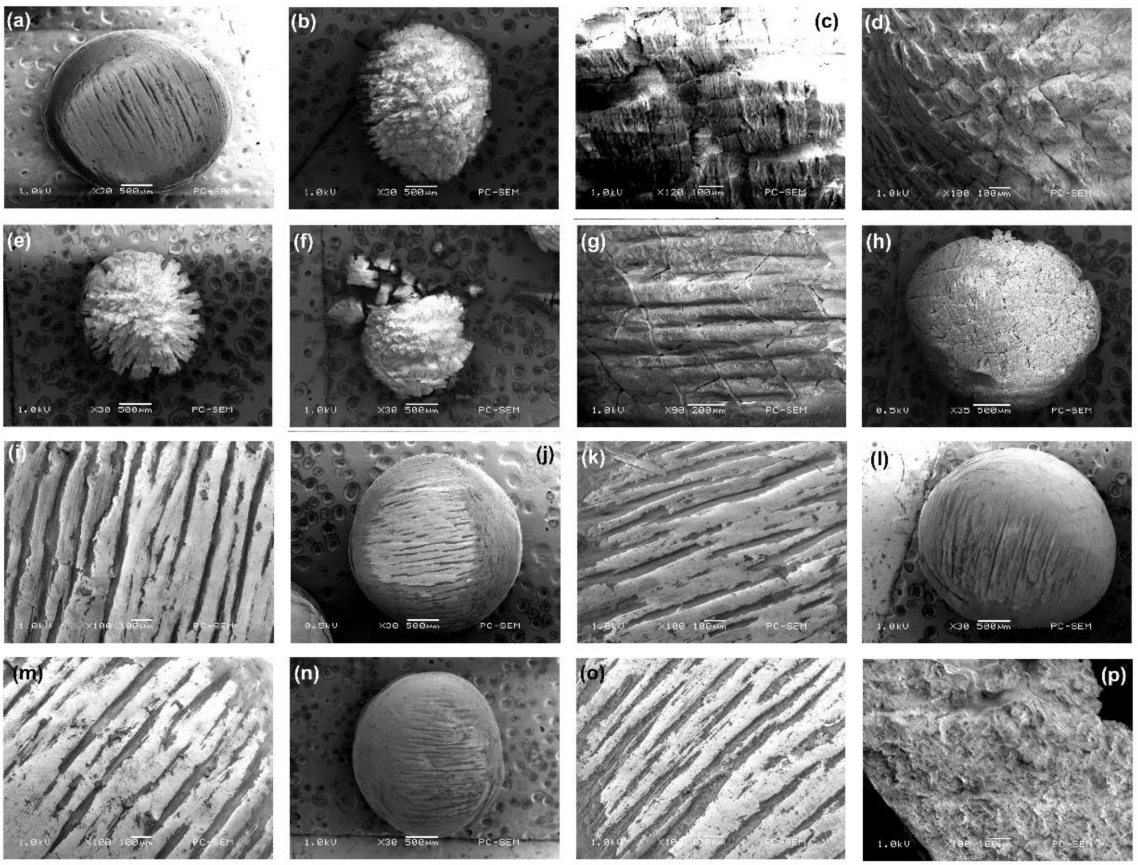

FIGURE 1 | **(A)** A virgin plastic pellet 30x. **(B)** Sunlight exposure 1.5 years, 30x. **(C)** Sunlight exposure 1.5 years, 120x. **(D)** Sunlight exposure 2 years, 120x. **(E)** Sunlight exposure 3 years, 30x. **(F)** Sunlight exposure 3.5 years, 30x. **(G)** UV 1.5 years, 90x. **(H)** UV 1.5 years, 35x **(I)** Seawater with sodium azide under sunlight exposure 1.5 years, 100x. **(J)** Seawater with sodium azide under sunlight exposure 3 years, 30x. **(K)** Seawater and sunlight exposure 1.5 years, 120x. **(L)** Seawater and sunlight exposure 3 years, 30x. **(M)** UV exposed seawater with sodium nitride 1.5 years, 100x. **(N)** UV exposed seawater with sodium nitride 3 years, 30x. **(O)** Oven at 100°C 0.5 years, 100x. **(P)** Oven at 100°C 2.5 years, 100x.

representation of the linear slope, using the Single Case Research Calculator. The Kruskal-Wallis test, a non-parametric equivalent of ANOVA used Vassarstats Net, with test statistic *H*. Throughout we have accepted test statistics where they met a 95% confidence level, and p values are listed in the text.

RESULTS AND DISCUSSION

Scanning Electron Microscopy

Scanning electron micrographs at a magnification of 30-120x reveal a range of different degradation patterns (**Figure 1** and electronic **Supplementary Figures SI-1, SI-2**). A new, spherical virgin pellet (V) is shown in **Figure 1A**, which is around 3 mm in diameter and weighs about 18 mg. The micrograph reveals characteristic striations that represent valleys of varying depth left during manufacture, typically some 600-900 μm in length and separated by 100-200 μm. The particle changes dramatically after sunlight irradiation. Over 1.5 years, particles become smaller (typically ~ 2.5 mm), losing material, and as shown in **Figure 1B**. The surface is indented with deep cracks that form knobby, yet angular features as "islands", some 100 μm across. The size suggests that the cracks have formed at the scale of the original striations. Higher magnification (**Figure 1C**) shows finer level cracking with a spacing of about 15-30 μm. After three years the cracks penetrate even more deeply into the pellet (**Figures 1D, E**) and the size has decreased further (~1.27 mm) and by 3.5 years (**Figure 1F**), the pellets are so degraded they begin to fragment and separate into flat sided spherical sectors with dimensions up to several hundred microns across. Degradation under UV reveals fine cracks (**Figure 1G**) after 1.5 years that run across the original striations and are separated by about 200 μm; leading after further exposure to a crazed surface to the pellet (**Figure 1H**). In other samples larger cracks align with striations, but damage under UV is limited to the surface as noted by Wu et al. (2011), who observed that chain scission of POM under UV irradiation was constrained within 100 μm of the surface. Photo degradation resulted in the cracks

forming on the surface gradually extending to the interior, and sunlight resulted in stronger fragmentation than UV-B, due to a control by oxygen diffusion or by penetration of UV light, and can be limited in the bulk (Masry et al., 2021). In the case where a plastic is exposed to the same external conditions, the surface degradation should increase with the UV or sunlight irradiation exposure time, and similar results were found in polyvinyl chloride and polypropylene (Tang et al., 2018; Tang et al., 2019; Masry et al., 2021).

Pellet exposure to seawater with sodium azide under sunlight (**Figures 1I, J**), also seawater and sunlight exposure (**Figures 1K, L**) and UV exposed seawater with sodium azide (**Figures 1M, N**) show little surface change, the seawater and perhaps biofilms, offering some degree of protection as has been noted with polyvinyl chloride and polypropylene (Tang et al., 2018; Tang et al., 2019; Masry et al., 2021). Furthermore, the slower degradation rate in water may also be due to air having higher oxygen content, UV transmittance and higher temperature as compared with water (Pimentel et al., 2005; Andrady, 2011; Cai et al., 2018; Tang et al., 2018; Biber et al., 2019; Ranjan and Goel, 2019; Tang et al., 2019; Masry et al., 2021). High temperature exposures (**Figures 1O, P**) show no change until the pellets melt and reveal an amorphous appearance.

Particle Fragmentation

The size change of pellets over time under various conditions is shown in **Figure 2A**. Sunlight irradiation causes an obvious reduction in the pellet diameter which amounts to about -570 μm years^{-1}, determined from the Theil-Sen slope. The Kendall rank coefficient (τ=-0.91; n=18) shows the decrease to be significant (p<.0001). UV irradiation and UV irradiation of the particles in seawater in the presence of azide also shows a decrease in pellet diameter -147 and -95 μm years^{-1}, again significant from Kendall's test (τ=-0.7; p<.0002 and τ=-0.5; p=~.003). There is a slight decrease in diameter from the samples placed in an oven: 34 μm years^{-1} (τ=-0.35; p=~.05). The other exposures, plotted as black dots, revealed no significant change in pellet diameter (p>.15). The degraded plastic remains white, although under

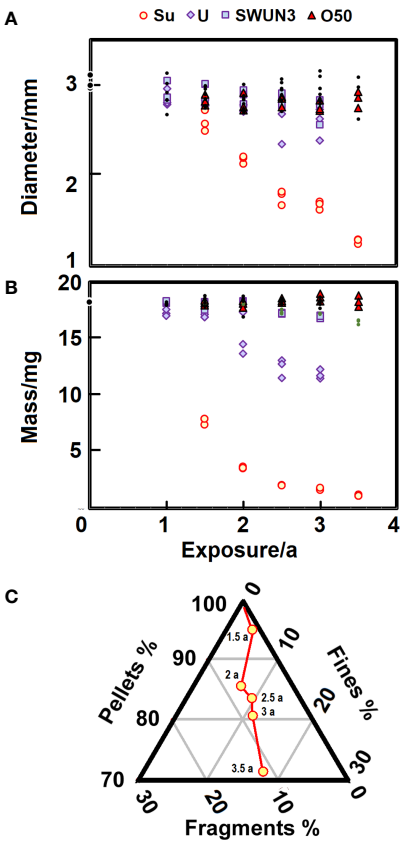

FIGURE 2 | **(A)** Change in diameter of particles under various types of exposure. The black dots include exposures POM_SwSuNa, POM_SWSu and POM_SwNa, which show no statistically significant change. **(B)** Mass loss from particles under various types of exposure. The black dots include exposures POM_SWSu and POM_SwNa, although in this figure POM_SwSuNa are shown as dots of a lighter shade (green dots). **(C)** The fraction of particles in three size ranges as they are exposed up to 3.5 years.

solar irradiation in the seawater, where the azide biocide was absent.

The pellets clearly fragment especially under solar illumination, so it is hardly surprising that they lose mass as they age (**Figure 2B**) in addition to the shrinkage alluded to earlier. POM is well known for experiencing tens of percent mass loss during thermal ageing (Fayolle et al., 2008; Li et al., 2019) and when under stress (Parrington, 2002). As expected from the measurements of particle diameter the pellets under sunlight irradiation rapidly lose mass. Over the first year and a half the particles shed some 11 mg of the mass, i.e. almost 60%. So much is lost that it takes on an exponential form, and unsurprisingly Kendall's test reveals high significance for the changes (τ=-0.95; p<.0001; n=18). After three years the particles are around a milligram, just 10% of their original mass. Decreasing mass is also evident from particles under UV irradiation which lose about 2.24 mg a^{-1} (τ=-0.83; p<.0001), but the other degradation processes show little convincing change, although there may have been some hints of slow (0.57 mg a^{-1}), though statistically significant (τ=-0.81; p<.0001) mass loss from the sample exposed in seawater under sunlight irradiation in the presence of azide. This would have reduced any biofilm formation (samples POM_SwSuNa). However, many of the pellets are the same size and mass, though a few are highly degraded.

The fragmentation of a pellet under sunlight irradiation for more than three years yields pieces some hundred microns across (**Figure 1F**). These derive from cracks that penetrate radially inward, developing over the first 1.5 a to ~225 μm although nine measurements from the five exposure times show little subsequent change (Kruskal-Wallis H=3.5; dof=4; p~.48), with the median for the 45 measurements of crack penetration 224; $Q_{1\ =}$ 212; $Q_{3\ =}$ 263 μm. The fragments seem to take on characteristic dimensions, set perhaps by the original striations on the pellet, so sieves of 297 and 177 μm proved convenient to separate the degraded plastic. This

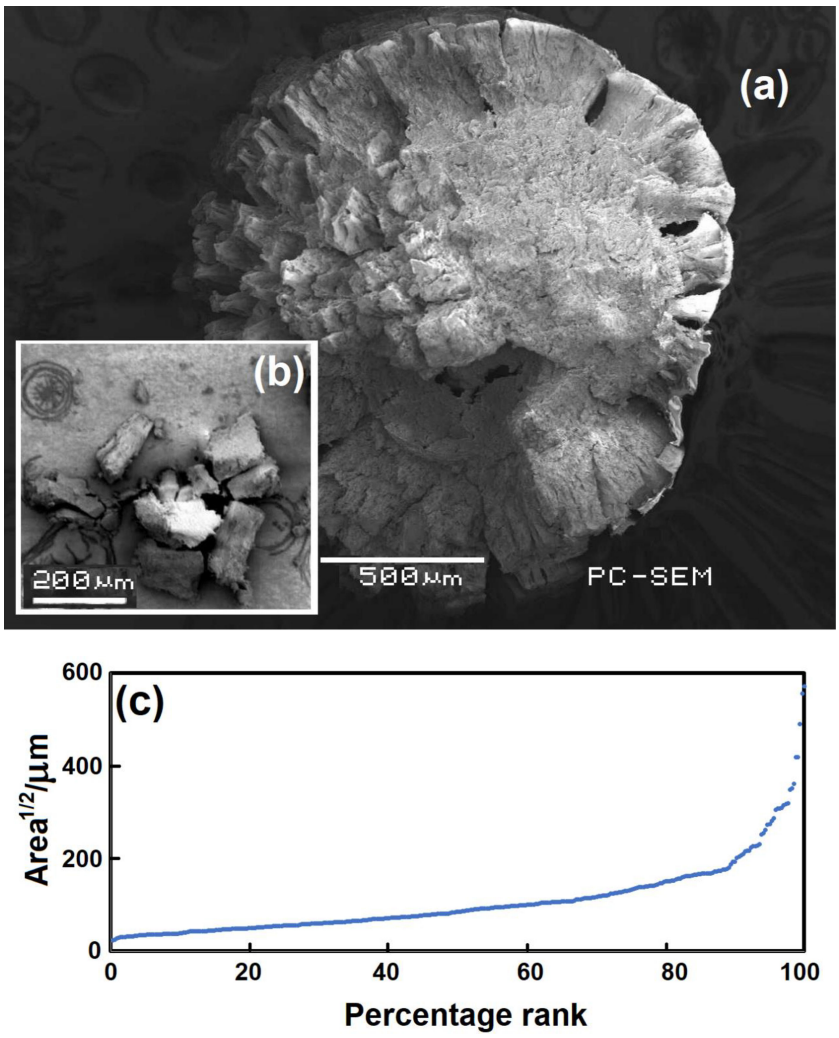

FIGURE 3 | **(A)** Pellet split in half after exposure to sunlight for 3.5 years. **(B)** Typical fragments, which separate after sunlight exposure. **(C)** Ranked dimension of fragments separating from pellets exposed to sunlight.

size was noted by Conkle et al. (2018) who argue that an important portion of marine plastic <300 μm in diameter was often neglected in surveys. The mass fractions in the three size classes (*pellets* >297 μm, *fragments* 297-177 μm and *fines* <177 μm), over time are shown as a ternary plot in **Figure 2C** for sunlit conditions. The triangle represents only a small part of the complete ternary diagram, to make the growing amount of finer material more obvious. It is evident under sunlight illumination that the larger fragments grow at first, but there are increasing amounts of fines <177 μm. The other degradation modes reveal much less fragmentation to finer material, the UV exposure being the most pronounced. After three years ~0.13% are fragments and 0.91% are fines, with 99% of the mass remaining as the pellets.

As the pellets degrade, they develop features at the surface that resemble broccoli florets (**Figure 3A**) that extend to a depth of 100 μm or more. Some 80% of visible light across the wavelength range 400-2000 nm is transmitted through a 15 μm POM film (Whittet et al., 1976), so sunlight penetration into the particles is likely, allowing these to break away as fragments shown in **Figure 3B**. We determined the areas of these using *Image J* for the sunlight exposures, examining almost 350 fragments ranging from 0.5-325x10^{-9} m^{-2}. This was converted to a dimension representative of an idealized square by taking the square root of the area. The Kruskal-Wallis test suggested little difference in the size of the fragments from various exposure times in sunlight (H=4.4; df=4; p~.35). In contrast to sunlight, UV radiation which interacts with the polymer is likely to be absorbed near the surface of the pellet (Wu et al., 2011), hence the concentration of degradation features at the surface (**Figure 1H**).

Photo degradation can lead to cracks on the surface which propagate deeper into the plastic and cause the plastic to split into two or more fragments. Fragments sizes varied overall from 30 nm to 1000 μm, and the particle size distribution showed an increase in particle concentration with decreasing particle size (Masry et al., 2021). The fragmentation process described here is more extensive than parallel studies of the weathering of polyvinylchloride or polypropylene pellets, and the fragmentation rate and generated particle sizes depends on the polymer type, shape, composition and external conditions (Tang et al., 2018; Tang et al., 2019; Masry et al., 2021). POM degradation would occur more rapidly in sunlit water to produce fragments where ~95% are likely to be <300 μm (**Figure 3C**). These smaller sizes are important as they are easily ingested by fish. Particles >100 μm are almost five times more likely to be ingested by fish than larger particles of >500 μm (Jovanović, 2017). The degraded POM fragments are also in the size encountered in natural turbidite systems, where 90% of the particles are <214 μm (Pohl et al., 2020), so POM fragments are likely to become associated with turbidity currents in sediments. On the other hand, as fragment size decreases, ingestion by a wide diversity of organisms is favored (Masry et al., 2021).

Fourier Transform Infrared Spectroscopy

The infrared spectra (**Figure 4A**) show that the main changes under weathering relate to the OH bond at 3398 cm^{-1}. The changes in OH absorbance as a function of age is shown in **Figure 4B**. Under sunlight irradiation we see an increase in the OH absorption until the particle begins to fragment after 3.5 years. In the case of UV irradiation after a rapid increase in OH intensity in the first year it stabilizes at more modest values, so although OH seems to increase it appears to be lost as weathering proceeds to its final stages. These changes are mirrored in the physical alteration to the pellets and illustrated in the reduction of their diameter as shown in **Figure 4C**. Links between observable change and the spectra were noted in earlier work especially during the first year of PVC and PP exposure (Tang et al., 2018; Tang et al., 2019). As a result, the formation of oxidation products leads to modifications of the infrared spectrum of the polymer. Identification and quantification of the oxidation products are essential for understanding of the mechanism of

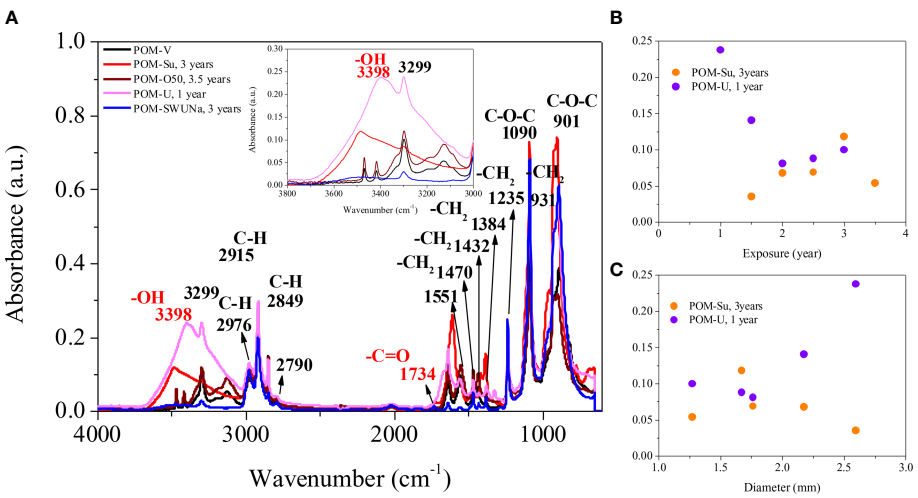

FIGURE 4 | **(A)** FTIR of some of the virgin and weathered plastic pellets, with an inset enlarging the region of the -OH group. **(B)** Peak height of OH as a function of pellet exposure in sunlight and UV. **(C)** Peak height of OH as a function of pellet diameter for the sunlit and UV weathering regimes.

degradation and to determine the weathering extent of plastic debris (Masry et al., 2021). The main photodegradation products of polyoxymethylene: H2CO, CO, HCOOH, O2, CH3OH, CH3OCHO, CH3OCH3OCH3 and C3H6O3 (trioxane) were identified (Cottin et al., 2000). These products may be released to the marine environment with POM weathering.

Environmental Implication

Solar and UVB degradation resulted in severe eroding behavior and reflected by cracking and the formation of hydroxyl functional groups on the surface of eroded polyoxymethylene (POM) pellets, an emerging plastic pollutant in runoff. These are new scientific findings, and the altered morphology and chemical properties could explain the affinity of plastic marine debris for trace metals, persistent organic pollutants, and microbes, as well as their tendency for biofouling.

CONCLUSIONS

Polyoxymethylene pellets in sunlight degrade *via* surface cracking to particles in the 100-300 μm range that are of similar dimension to the striations seen on the surface of the original particles. The polyoxymethylene pellets subsequently fragment to finer material, especially on exposure to sunlight. Photodegradation reveals increases in OH bonds on the pellet surface. Physical changes, such as reduction in diameter or fragmentation mirror the magnitude of changes in the FTIR spectra. Future work should extend to macroplastics and other polymers, to gain a sense of how they are likely to degrade to smaller fragments in realistic marine environments and explore whether seawater and biofilms retard degradation. The work adds to evidence that finer plastics in the environment are underestimated because the fraction below 300 μm may go unrecorded.

DATA AVAILABILITY STATEMENT

The original contributions presented in the study are included in the article/**Supplementary Material**. Further inquiries can be directed to the corresponding author.

AUTHOR CONTRIBUTIONS

All, review and editing. C-LL and H-IC, conceptualization, methodology, and supervision. C-CT, investigation, original draft preparation and visualization. Y-TC and Y-MZ, investigation and image analysis. PB, formal analysis, writing and visualization. All authors contributed to the article and approved the submitted version.

FUNDING

This work was supported by grants from the Ministry of Science and Technology (MOST) and the Ministry of Education of Taiwan, ROC, under Contract Numbers MOST 107-2611-M-110-008, MOST108-2611-M-110-008 and DOE 01C030703.

SUPPLEMENTARY MATERIAL

The Supplementary Material for this article can be found online at: https://www.frontiersin.org/articles/10.3389/fmars.2022.843295/full#supplementary-material

REFERENCES

Alimi, O. S., Farner Budarz, J., Hernandez, L. M., and Tufenkji, N. (2018). Microplastics and Nanoplastics in Aquatic Environments: Aggregation, Deposition, and Enhanced Contaminant Transport. *Environ. Sci. Technol.* 52, 1704–1724. doi: 10.1021/acs.est.7b05559

Andrady, A. L. (2011). Microplastics in the Marine Environment. *Mar. Pollut. Bull.* 62, 1596–1605. doi: 10.1016/j.marpolbul.2011.05.030

Bakir, A., Rowland, S. J., and Thompson, R. C. (2014). Enhanced Desorption of Persistent Organic Pollutants From Microplastics Under Simulated Physiological Conditions. *Environ. Pollut.* 185, 16–23. doi: 10.1016/j.envpol.2013.10.007

Barletta, M., Lima, A. R. A., and Costa, M. F. (2019). Distribution, Sources and Consequences of Nutrients, Persistent Organic Pollutants, Metals and Microplastics in South American Estuaries. *Sci. Total. Environ.* 651, 1199–1218. doi: 10.1016/j.scitotenv.2018.09.276

Biber, N. F. A., Foggo, A., and Thompson, R. C. (2019). Characterising the Deterioration of Different Plastics in Air and Seawater. *Mar. Pollut. Bull.* 141, 595–602. doi: 10.1016/j.marpolbul.2019.02.068

Cai, L., Wang, J., Peng, J., Wu, Z., and Tan, X. (2018). Observation of the Degradation of Three Types of Plastic Pellets Exposed to UV Irradiation in Three Different Environments. *Sci. Total Environ.* 628–629, 740–747. doi: 10.1016/j.scitotenv.2018.02.079

Carbery, M., O'Connor, W., and Palanisami, T. (2018). Trophic Transfer of Microplastics and Mixed Contaminants in the Marine Food Web and Implications for Human Health. *Environ. Int.* 115, 400–409. doi: 10.1016/j.envint.2018.03.007

Conkle, J. L., Del Valle, C. D. B., and Turner, J. W. (2018). Are We Underestimating Microplastic Contamination in Aquatic Environments? *Environ. Manage.* 61 (1), 1–8. doi: 10.1007/s00267-017-0947-8

Cottin, H., Gazeau, M.-C., Doussin, J.-F., and Raulin, F. (2000). An Experimental Study of the Photodegradation of Polyoxymethylene at 122, 147 and 193 Nm. *J. Photochem. Photobiol. A* 135, 53–64. doi: 10.1016/S1010-6030(00)00274-4

Coyle, R., Hardiman, G., and Driscoll, K. O. (2020). Microplastics in the Marine Environment: A Review of Their Sources, Distribution Processes and Uptake Into Ecosystems. *Case Stud. Chem. Environ. Eng.*, 100010. doi: 10.1016/j.cscee.2020.100010

Fayolle, B., Verdu, J., Bastard, M., and Piccoz, D. (2008). Thermooxidative Ageing of Polyoxymethylene, Part 1: Chemical Aspects. *J. Appl. Polym. Sci.* 107 (3), 1783–1792. doi: 10.1002/app.26648

Fotopoulou, K. N., and Karapanagioti, H. K. (2017). "Degradation of Various Plastics in the Environment," in *Hazardous Chemicals Associated With Plastics in the Marine Environment* (Cham: Springer), 71–92. doi: 10.1007/698_2017_11

Gangadoo, S., Owen, S., Rajapaksha, P., Plaisted, K., Cheeseman, S., Haddara, H., et al. (2020). Nano-Plastics and Their Analytical Characterisation and Fate in the Marine Environment: From Source to Sea. *Sci. Total Environ.* 732, 138792. doi: 10.1016/j.scitotenv.2020.138792

Gilpin, A. R. (1993). Table for Conversion of Kendall's Tau to Spearman's Rho Within the Context Measures of Magnitude of Effect for Meta-Analysis. *Educ. Psychol. Meas.* 53, 87–92. doi 10.1177/0013164493053001007.

Hahladakis, J. N., Velis, C. A., Weber, R., Iacovidou, E., and Purnell, P. (2018). An Overview of Chemical Additives Present in Plastics: Migration, Release, Fate and

Environmental Impact During Their Use, Disposal and Recycling. *J. Hazard. Mater.* 344, 179–199. doi 10.1016/j.jhazmat.2017.10.014.

Hermabessiere, L., Dehaut, A., Paul-Pont, I., Lacroix, C., Jezequel, R., Soudant, P., et al. (2017). Occurrence and Effects of Plastic Additives on Marine Environments and Organisms: A Review. *Chemosphere* 182, 781–793. doi 10.1016/j.chemosphere.2017.05.096.

Image J. Available at: https://imagej.nih.gov/ij/index.html.

Huffer, T., Weniger, A. K., and Hofmann, T. (2018). Sorption of Organic Compounds by Aged Polystyrene Microplastic Particles. *Environ. Pollut.* 236, 218–225. doi 10.1016/j.envpol.2018.01.022.

Jovanović, B. (2017). Ingestion of Microplastics by Fish and Its Potential Consequences From a Physical Perspective. *Integr. Environ. Assess. Manage.* 13 (3), 510–515. doi: 10.1002/ieam.1913

Kavya, A. N. L., Sundarrajan, S., and Ramakrishna, S. (2020). Identification and Characterization of Micro-Plastics in the Marine Environment: A Mini Review. *Mar. Pollut. Bull.* 160, 111704. doi 10.1016/j.marpolbul.2020.111704.

Król-Morkisz, K., Karaś, E., Majka, T. M., Pielichowski, K., and Pielichowska, K. (2019). Thermal Stabilization of Polyoxymethylene by PEG-Functionalized Hydroxyapatite: Examining the Effects of Reduced Formaldehyde Release and Enhanced Bioactivity. *Adv. Polym. Technol.* 2019, 1–17. doi 10.1155/2019/9728637.

Kubecka, P.L. 2001. A Possible World Record Maximum Natural Ground Surface Temperature. *Weather 56*, 218–221. doi 10.1002/j.1477-8696.2001.tb06577.x.

Kusy, R. P., and Whitley, J. Q. (2005). Degradation of Plastic Polyoxymethylene Brackets and the Subsequent Release of Toxic Formaldehyde. *Am. J. Orthod. Dentofac. Orthop.* 127, 420–427. doi: 10.1016/j.ajodo.2004.01.023

Liu, S., Chen, H., Wang, J., Su, L., Wang, X., Zhu, J., et al. (2021). The Distribution of Microplastics in Water, Sediment, and Fish of the Dafeng River, a Remote River in China. *Ecotoxicol. Environ. Saf.* 228, 113009. doi: 10.1016/j.ecoenv.2021.113009

Li, J., Wang, Y., Wang, X., and Wu, D. (2019). Development of Polyoxymethylene/Polylactide Blends for a Potentially Biodegradable Material: Crystallization Kinetics, Lifespan Prediction, and Enzymatic Degradation Behavior. *Polymers* 11 (9), 1516. doi 10.3390/polym11091516.

Lüftl, S., Archodoulaki, V. M., and Seidler, S. (2006). Thermal-Oxidative Induced Degradation Behaviour of Polyoxymethylene (POM) Copolymer Detected by TGA/Ms. *Polym. Degrad. Stab.* 91 (3), 464–471. doi 10.1016/j.polymdegradstab.2005.01.029.

Masry, M., Rossignol, S., Gardette, J. L., Therias, S., Bussiere, P. O., and Wong-Wah-Chung, P. (2021). Characteristics, Fate, and Impact of Marine Plastic Debris Exposed to Sunlight: A Review. *Mar. Pollut. Bull.* 171, 14. doi: 10.1016/j.marpolbul.2021.112701

Mildrexler, D. J., Zhao, M. S., and Running, S. W. 2011. Satellite Finds Highest Land Skin Temperatures on Earth. *Bull. Amer. Meteorol. Soc. 92*, 855–860. doi doi: 10.1175/2011BAMS3067.1.

Min, K., Cuiffi, J. D., and Mathers, R. T. (2020). Ranking Environmental Degradation Trends of Plastic Marine Debris Based on Physical Properties and Molecular Structure. *Nat. Commun.* 11 (1), 1–11. doi 10.1038/s41467-020-14538-z.

Naik, R. A., Rowles, L. S.3rd, Hossain, A. I., Yen, M., Aldossary, R. M., Apul, O. G., et al. (2020). Microplastic Particle Versus Fiber Generation During Photo-Transformation in Simulated Seawater. *Sci. Total. Environ.* 736, 139690. doi 10.1016/j.scitotenv.2020.139690.

Napper, I. E., and Thompson, R. C. (2020). Plastic Debris in the Marine Environment: History and Future Challenges. *Glob. Chall.* 4, 1900081. doi: 10.1002/gch2.201900081

Parrington, R. J. (2002). Fractography of Metals and Plastics. *Pract. Failure Anal.* 2 (5), 16–19. doi 10.1002/gch2.201900081.

Pimentel, L. R., Gardette, J.-L., and Pereira Rocha, A. (2005). Artificial Simulated and Natural Weathering of Poly(Vinyl Chloride) for Outdoor Applications: The Influence of Water in the Changes of Properties. *Polym. Degrad. Stab.* 88, 357–362. doi: 10.1016/j.polymdegradstab.2004.11.012

Plummer, C. J. (2004). "Microdeformation and Fracture in Bulk Polyolefins," in *Long Term Properties of Polyolefins* (Berlin, Heidelberg: Springer), 75–120. Available at: doi 10.1007/b13520.

Plummer, C. J., Scaramuzzino, P., Kausch, H. H., and Philippoz, J. M. (2000). High Temperature Slow Crack Growth in Polyoxymethylene. *Polym. Eng. Sci.* 40 (6), 1306–1317. doi 10.1002/pen.11259.

Pohl, F., Eggenhuisen, J. T., Kane, I. A., and Clare, M. A. (2020). Transport and Burial of Microplastics in Deep-Marine Sediments by Turbidity Currents. *Environ. Sci. Technol.* 54 (7), 4180–4189. doi: 10.1021/acs.est.9b07527

Rabek, J. F. (2012). *Polymer Photodegradation: Mechanisms and Experimental Methods* (London, UK: Springer Science & Business Media). Available at: doi 10.1007/978-94-011-1274-1.

Ranjan, V. P., and Goel, S. (2019). Degradation of Low-Density Polyethylene Film Exposed to UV Radiation in Four Environments. *J. Hazard. Toxic Radioact. Waste* 23, 04019015. doi: 10.1061/(ASCE)HZ.2153-5515.0000453

Royer, S. J., Ferrón, S., Wilson, S. T., and Karl, D. M. (2018). Production of Methane and Ethylene From Plastic in the Environment. *PloS One* 13 (8), e0200574. doi 10.1371/journal.pone.0200574.

Sfriso, A. A., Tomio, Y., Rosso, B., Gambaro, A., Sfriso, A., Corami, F., et al. (2020). Microplastic Accumulation in Benthic Invertebrates in Terra Nova Bay (Ross Sea, Antarctica). *Environ. Int.* 137, 105587. doi 10.1016/j.envint.2020.105587.

Single Case Research Calculator. Available at: http://www.singlecaseresearch.org/calculators/theil-sen.

Song, Y. K., Hong, S. H., Jang, M., Kang, J. H., Kwon, O. Y., Han, G. M., et al. (2014). Large Accumulation of Micro-Sized Synthetic Polymer Particles in the Sea Surface Microlayer. *Environ. Sci. Technol.* 48, 9014–9021. doi 10.1021/es501757s.

Tang, C. C., Chen, H. I., Brimblecombe, P., and Lee, C. L. (2018). Textural, Surface and Chemical Properties of Polyvinyl Chloride Particles Degraded in a Simulated Environment. *Mar. Pollut. Bull.* 133, 392–401. doi 10.1016/j.marpolbul.2018.05.062.

Tang, C. C., Chen, H. I., Brimblecombe, P., and Lee, C. L. (2019). Morphology and Chemical Properties of Polypropylene Pellets Degraded in Simulated Terrestrial and Marine Environments. *Mar. Pollut. Bull.* 149, 110626. doi 10.1016/j.marpolbul.2019.110626.

Thompson, R. C., Olsen, Y., Mitchell, R. P., Davis, A., Rowland, S. J., John, A. W. G., et al. (2004). Lost at Sea: Where Is All the Plastic? *Science* 304 (5672), 838–838. doi: 10.1126/science.1094559

Vassarstats Net. Available at: http://vassarstats.net/.

Vilà Ramirez, N., Sanchez-Soto, M., Illescas, S., and Gordillo, A. (2009). Thermal Degradation of Polyoxymethylene Evaluated With FTIR and Spectrophotometry. *Polym. Plast. Technol. Eng.* 48, 470–477. doi 10.1080/03602550902725472.

Wang, F., Wong, C. S., Chen, D., Lu, X., Wang, F., and Zeng, E. Y. (2018). Interaction of Toxic Chemicals With Microplastics: A Critical Review. *Water. Res.* 139, 208–219. doi 10.1016/j.watres.2018.04.003.

Webb, H., Arnott, J., Crawford, R., and Ivanova, E. (2012). Plastic Degradation and Its Environmental Implications With Special Reference to Poly(ethylene Terephthalate). *Polymers* 5, 1–18. doi 10.3390/polym5010001.

Wessa.Net. Available at: https://www.wessa.net/stat.wasp.

Whittet, D. C. B., Dayawansa, I. J., Dickinson, P. M., Marsden, J. P., and Thomas, B. (1976). The Optical Constants of Polyoxymethylene. *Mon. Not. R. Astron. Soc.* 175 (1), 197–207. doi 10.1093/mnras/175.1.197.

Wu, G., Lu, C., Cai, X., and Ren, X. (2011). Mechanical Properties and Solid-State Structure of Photodegraded Polyoxymethylene and Effect of UV Stabilizers Modification. *J. Macromol. Sci Part B* 50 (8), 1521–1534. doi 10.1080/00222341003775830.

Zhang, W., Xu, X., Wei, F., Zou, X., and Zhang, Y. (2018). Influence of Dielectric Barrier Discharge Treatment on Surface Structure of Polyoxymethylene Fiber and Interfacial Interaction With Cement. *Materials* 11 (10), 1873. doi 10.3390/ma11101873.

Conflict of Interest: The authors declare that the research was conducted in the absence of any commercial or financial relationships that could be construed as a potential conflict of interest.